J|A|C|S
ARTICLES

Published on Web 09/23/2009

Nucleation Kinetics vs Chemical Kinetics in the Initial Formation of Semiconductor Nanocrystals

Renguo Xie, Zheng Li, and Xiaogang Peng*

Department of Chemistry and Biochemistry, University of Arkansas, Fayetteville, Arkansas 72701

Received July 28, 2009; E-mail: xpeng@uark.edu

Abstract: The initial formation of semiconductor nanocrystals/nanoclusters, that is, nucleation in the classic literature, was examined both theoretically and experimentally. An experimental method based on determining the initial reaction rate for the formation of nanocrystals/nanoclusters with fixed size and size distribution was developed using InP and CdS nanocrystals/nanoclusters systems, especially the InP one. This experimental strategy relies on the size-dependent absorption spectra of these semiconductor nanoparticles as quantitative probes. The experimental results along with theoretical analysis indicate that the classic nucleation model was unlikely relevant for such crystallization systems, whose bulk crystal solubility in a solution is extremely low. Instead, the formation process was found to match a reaction-controlled kinetics model. The results further imply that understanding of crystallization and development of controlled synthesis of high quality colloidal nanocrystals are both closely related to identifying the molecular mechanism and chemical kinetics.

Introduction

Crystallization is one of few most interesting yet mysterious phenomena to human beings. The recent interest in nanocrystals and other types of nanomaterials further illustrates the importance of understanding crystallization in science and technology.[1−4] In literature, nucleation refers to the initial formation process of a crystal phase from another phase, usually a liquid, a solution, or a gas phase. Nucleation defines the boundary conditions for a given crystallization system and thus likely dictates the following growth process under given temperature and pressure. Unfortunately, study of nucleation process is a grand challenge mostly because of the difficulty to quantitatively determine the size and concentration of the newly formed tiny clusters/nanocrystals.[5,6] Quantum confined semiconductor nanoclusters/nanocrystals (q-dots) are well-known for their strongly size dependent optical properties in the size regime from a few atoms to several millions of atoms.[7] This work intends to establish a method for studying the related nucleation processes of q-dots. The experimental results from two q-dots systems, InP (the main one) and CdS ones, were examined against the theoretical models explored in this work.

The classic theory of crystallization in solution is largely built on the fact that the solubility of a crystal with defined lattice structure and composition increases drastically in the nanometer size regime, which is quantitatively expressed as the Gibbs−Thompson equation (see below).[5,6] In this classic picture, the continuous growth in size of crystals can only occur if the size of the initial crystal embryo is larger than a given value, which are called critical sized nuclei. In the solution, any crystals smaller than the critical sized nuclei possess a thermodynamic tendency to dissolve and any crystals larger than the critical sized nuclei shall be thermodynamically driven to grow. This inspired a kinetics model for nucleation proposed by Gibbs, with the free energy difference between the monomers in solution and the critical sized nuclei as the activation free energy. Though this model has been widely adopted in literature, it often showed at least a few magnitudes of difference from experimental results.[5,6,8]

Thus, the theoretical challenge for understanding nucleation is well-known to the field. However, lack of reliable and systematic experimental data in the early stage of a crystallization system implies that there are no sufficient insights for solving such a challenge. In the field of colloidal nanocrystals, scientists have started to pay attention to the nucleation stage.[9−11] However, to our knowledge, systematic and quantitative studies on nucleation of colloidal nanocrystals are yet to emerge, which requires systematic variation of reaction temperature and reactant concentrations. Specifically for semiconductor nanocrystals, their unique size-dependent optical properties offer unique probes for studying crystallization as mentioned above. However, these studies are largely on the

(1) Murray, C. B.; Kagan, C. R.; Bawendi, M. G. *Annu. Rev. Mater. Sci.* **2000**, *30*, 545–610.
(2) Tian, Z. R.; Voigt, J. A.; Liu, J.; McKenzie, B.; McDermott, M. J.; Rodriguez, M. A.; Konishi, H.; Xu, H. *Nat. Mater.* **2003**, *2*, 821–826.
(3) Xia, Y. N.; Yang, P. D.; Sun, Y. G.; Wu, Y. Y.; Mayers, B.; Gates, B.; Yin, Y. D.; Kim, F.; Yan, Y. Q. *Adv. Mater.* **2003**, *15*, 353–389.
(4) Peng, X. G. *Nano Res.* **2009**, *2*, 425–447.
(5) Mullin, J. W. *Crystallization*, 3rd ed.; 1997.
(6) Oxtoby, D. W. *Acc. Chem. Res.* **1998**, *31*, 91–97.
(7) Brus, L. E. *J. Chem. Phys.* **1984**, *80*, 4403–4409.
(8) Erdemir, D.; Lee, A. Y.; Myerson, A. S. *Acc. Chem. Res.* **2009**, *42*, 621–629.
(9) Qu, L.; Yu, W. W.; Peng, X. *Nano Lett.* **2004**, *4*, 465–469.
(10) Kwon, S. G.; Piao, Y.; Park, J.; Angappane, S.; Jo, Y.; Hwang, N. M.; Park, J. G.; Hyeon, T. *J. Am. Chem. Soc.* **2007**, *129*, 12571–12584.
(11) Rempel, J. Y.; Bawendi, M. G.; Jensen, K. F. *J. Am. Chem. Soc.* **2009**, *131*, 4479–4489.

growth of the nanocrystals, and there are still plenty of challenges for one to quantitatively probe a nucleation process.[4]

This work designed a series of experiments mostly for the InP q-dots system in hopes of answering a few fundamental questions quantitatively on nucleation, or more precisely, formation of InP nanoclusters/nanocrystals. These questions include the validity of critical size nuclei, the effects of monomer concentration, the effects of ligands and other additives, and the effects of temperature. The key feature of the experimental method is to enable quantitative measurements by generating nanoclusters/nanocrystals with fixed size and size distribution in a reasonably broad experimental window. A theoretical section will be presented to examine options for understanding the experimental data to be described.

Theoretical Section

Classic Nucleation Theory. The classic nucleation theory has its roots in the Gibbs−Thompson equation (eq 1). In this subsection, we will try to discuss an approach different from the most popular one presented in literature which was originally derived by Gibbs.[5,6] Because of the increased surface-to-volume ratio, the chemical potential of a crystal increases rapidly as its size decreases. Consequently, its solubility increases as its size decreases following the Gibbs−Thompson equation (eq 1).

$$S_d = S_\infty \exp(4\,\sigma v_m/dRT) \tag{1}$$

where S_d and S_∞ are the solubility values of a crystal with its size (or diameter) as d and the corresponding bulk crystal, respectively. σ is the specific surface energy, and v_m is the molar volume of the crystal. R is the gas constant, and T is the absolute temperature. The Gibbs−Thompson equation assumes a spherical shape for crystals, which will be adopted in most parts of this work unless it is pointed out otherwise.

Thermodynamically speaking, eq 1 tells us that the chemical potential of a given-sized crystal equals to that of the monomers with their concentration being the solubility of the crystal.[12] This means that if μ_d and μ^o are, respectively, the chemical potential of a crystal with its size as d and the standard chemical potential of the monomers under the given conditions, we should have the following relationship.

$$\mu_d = \mu^o + RT\ln S_d = \mu^o + RT(\ln S_\infty + 4\sigma v_m/dRT) \tag{2}$$

For any monomer concentration represented as [M], the chemical potential of monomers in the solution (μ_M) can be expressed as eq 3.

$$\mu_M = \mu^o + RT\ln[M] \tag{3}$$

Formation of a crystal with its size as d from the monomers with their concentration being [M] shall involve a free energy change (ΔG) that should be calculated using eq 4. In eq 4, n is the total number of moles of the monomer units in the crystal, which is $\pi d^3/(6v_m)$ for the crystal with its size as d.

$$\Delta G = n(\mu_d - \mu_M) = \frac{\pi d^3 RT(\ln S_\infty + 4\sigma v_m/dRT - \ln[M])}{6v_m} = \frac{2\pi\sigma d^2}{3} - \frac{\pi d^3 RT\ln\omega}{6v_m} \tag{4}$$

Here, ω is defined as supersaturation, which is the ratio between the monomer concentration and the bulk solubility ($[M]/S_\infty$). In eq 4, the first term is positive. If ω is not greater than 1, ΔG will be always greater than zero and formation of crystals shall be thermodynamically prohibitive. Consequently, any crystals in the solution will dissolve. When ω is greater than 1, ΔG becomes negative when the size of the crystal is larger than the particles with its solubility equal to the given monomer concentration, whose size will be named d_e. At the same time, eq 4 tells us that, when $d = 0$, ΔG is also zero. Mathematically, one maximum shall exist between two nodes, d_e and $d = 0$. Let the derivative of ΔG equals to zero. This gives the critical sized nuclei (d^*) (eq 5) and the corresponding critical Gibbs free energy of nucleation (ΔG^*) as eq 6.

$$d^* = \frac{8\sigma v_m}{3RT\ln\omega} \tag{5}$$

$$\Delta G^* = \frac{128\pi\sigma^3 v_m^2}{(9RT\ln\omega)^2} \tag{6}$$

ΔG^* is considered as the activation free energy according to the Gibbs nucleation theory. Following the strategy proposed by Gibbs, the nucleation kinetics equation emerges as eq 7, provided that the particle concentration is defined as [P] and the formation rate of particles ($d[P]/dt$) is represented as r.

$$r = d[P]/dt = A\exp\frac{-128\pi\sigma^3 v_m^2}{(9\ln\omega)^2(RT)^3} \tag{7}$$

and

$$\ln(r) = \ln(A) - \frac{128\pi\sigma^3 v_m^2}{(9\ln\omega)^2(RT)^3} \tag{7a}$$

It should be pointed out that the most popular method to yield nucleation kinetics equations derived by Gibbs followed a geometric argument of the free energy change, which includes a positive term as the surface free energy and a negative term as the crystal interior part.[5,6] That method is direct, and the results are qualitatively the same as those presented in eqs 5−7. However, Gibbs equations are not self-consistent. For example, the crystal in equilibrium with the monomers in the solution, namely d_e, suggested by that model is different from the Gibbs−Thompson equation, although the method must apply the Gibbs−Thompson equation at some point in the deduction.[5] The resulting critical sized nuclei (d^*) in the Gibbs method is simply the crystal with its solubility equal to the monomer concentration in the solution (d_e) calculated from eq 1. This implies that either the Gibbs−Thompson equation or the classic nucleation kinetics equations should be modified. This work chose to stick to the Gibbs−Thompson equation simply because this equation has been widely accepted and used in fields of crystallization, surface science, etc. A more in depth theoretical argument is in development and shall be a part of a separate publication.

Quantitatively, the critical sized nuclei found in the Gibbs method are 1/3 larger in size (diameter) than the valve shown in eq 5. Although with this quantitative discrepancy, the main conclusion drawn in this report does not change using the equations obtained from either of the two methods.

Bulk Solubility. Bulk solubility, the term used in the above discussions, S_∞, needs to be clarified for determining ω, d^*, and

(12) Peng, Z. A.; Peng, X. *J. Am. Chem. Soc.* **2002**, *124*, 3343–3353.

ΔG^*, which is critically related to the solution conditions. By definition, it can be calculated from the solubility equilibrium constant (K_{sp}) of a given compound. Using InP as an example, the related chemical equilibrium should be as follows.

$$(InP)_{bulk} \leftrightarrow In^{3+} + P^{3-} \quad (8)$$

The K_{sp} of typical III−V and II−VI semiconductor compound is extremely small in aqueous solution. In nonpolar solutions, the ions are even more unstable. With the existence of ligands and other additives, however, the above equilibrium would be modified substantially. Typically, fatty acids (HFA) are common ligands, which shall establish a new equilibrium with InP crystals.

$$(InP)_{bulk} + 3HFA \leftrightarrow In(FA)_3 + H_3P \quad (9)$$

The chemical equilibrium constant for this equilibrium (eq 9) can be regarded as the K_{sp} observed in experiments, ${}^{obv}K_{sp}$.

$${}^{obv}K_{sp} = \frac{[In(FA)_3][H_3P]}{[HFA]^3} = [In^{3+}][P^{3-}]\bullet\frac{[H^+]^3[FA^-]^3}{[HFA]^3}\bullet\frac{[In(FA)_3]}{[In^{3+}][FA^-]^3}\bullet\frac{[H_3P]}{[H^+]^3[P^{3-}]} = \frac{K_{sp}\bullet({}^{HFA}K_a)^{3}\bullet{}^{In(FA)_3}K_s}{{}^{H_3P}K_a} \quad (10)$$

Here, ${}^{HFA}K_a$ and ${}^{H_3P}K_a$ are respectively the acid dissociation constants of HFA and H_3P, and ${}^{In(FA)_3}K_s$ is the complex stability constant of the indium fatty acid salt ($In(FA)_3$). Equation 10 implies that, in most experiments, ${}^{obv}K_{sp}$ is a complex combination of several chemical equilibrium constants, which is the thermodynamic root for the strong influence of solution environment on a crystallization system. This has recently been noticed both experimentally[13,14] and theoretically[11] in the field of colloidal nanocrystals.

Practically, solubility of a compound should be measured using a chosen component. In this report and the others related to the synthesis of high quality compound semiconductor nanocrystals, the cationic precursor is often in a large excess because the ligands are typical for the surface cations. Thus, it is more convenient to choose the anions as a measurement of the solubility. For InP system, we express the solubility of InP crystal using the concentration of the phosphors monomers. For simplicity, let us use H_3P as the representative of all possible phosphors monomers in the solution. From eqs 9 and 10, the solubility of bulk InP can be calculated using the following equation.

$$S_\infty = [H_3P] = {}^{obv}K_{sp}\frac{[HFA]^3}{[In(FA)_3]} = \frac{K_{sp}\bullet({}^{HFA}K_a)^{3}\bullet{}^{In(FA)_3}K_s}{{}^{H_3P}K_a}\bullet\frac{[HFA]^3}{[In(FA)_3]} \quad (11)$$

Equation 11 implies that, because of the direct dependence of the solubility (or chemical potential) of nanoclusters/nanocrystals on S_∞, a crystallization system must be considered by taking into account of the solution environment. It should be pointed out that although the specific surface free energy (σ) is known to be related to the possible surface adsorbents, the influence of solution environment on S_∞ is substantially more comprehensive. For example, related to the current system, the supersaturation should change substantially by varying the concentration of the fatty acid additives. This is so because the solubility of a given sized InP nanocluster/nanocrystal would increase dramatically—with a cubic function—by increasing the fatty acid concentration (eq 11). From a different perspective, the theoretical results in this subsection explain why ligands effects could be more substantial for monomers than that for the resulting nanocrystals.[14]

Limitations of Classic Nucleation Kinetics Model. The limitations of the classic nucleation kinetics model discussed above can be identified by going through the mathematic procedure. First, the Gibbs free energy barrier in eq 7 depends strongly on the monomer concentration, which is fundamentally different from the activation energy in chemical kinetics. Even if this model is correct, it is unlikely to identify a fixed size for critical sized nuclei and activation Gibbs free energy barrier (eqs 5 and 6), provided the rapid temporal change of the monomer concentration in practical synthesis. Second, the Gibbs free energy barrier identified by eq 6 is a thermodynamic barrier, instead of a kinetics barrier. It is quite possible that the formation of crystals may involve some common chemical reactions, such as formation of the structural unit (InP molecule in our example), the reaction occurred on the surface of a crystal embryo, and the diffusion of reactants, etc. As a result, if one of the chemical processes involved in nucleation is very slow, the entire nucleation might become reaction-controlled and the nucleation kinetics shown by eq 7 might not play much of a role at all.

From a pure thermodynamic standpoint, the nucleation kinetics presented above could have some significant limitations as well. This can be readily demonstrated by estimating the critical sized nuclei using eq 5.

There are barely any constants available to do such estimation in a practical nonaqueous synthetic system at this moment. For illustration of the principle, one can use an aqueous system to support the argument. Let us take the most common semiconductor nanocrystals, CdSe ones, as the example. The K_{sp} for CdSe is 6.3×10^{-36}. The K_a for typical fatty acids, such as acetic acid, and the K_a for H_2Se (the first- and second-step combined value) are 1.5×10^{-5} and 1.3×10^{-15}, respectively. The complex stability constant of cadmium fatty acid salt—cadmium acetate in this case—is found to be 1.4×10^3. The fatty acid concentration and cadmium fatty acid salt concentrations are both assumed to be 0.1 mol/L. For the specific surface free energy, let us take a relatively high end value used in the Talapin's report,[15] 0.5 J/m^2. This roughly corresponds to 50 000 J/mol for the free energy difference between a Se−Cd bond and a RCOO−Cd bond.

With all of the data offered in the above paragraph, one can calculate the size of the critical sized nuclei for CdSe in this specific system at 298 K to be 0.29 nm. This is slightly smaller than the length of a single Cd−Se bond, which means that the basis of nucleation kinetics does not exist at all. In other words, there appears to be no free energy barrier for the formation of CdSe crystals/clusters with any size, even if the clusters are $(CdSe)_2$ and $(CdSe)_3$. It should be pointed out that, under the acidity specified above, it is more proper for H_2Se to ionize

(13) Yu, W. W.; Peng, X. *Angew. Chemie, Int. Ed.* **2002**, *41*, 2368–2371.
(14) Yu, W. W.; Wang, Y. A.; Peng, X. *Chem. Mater.* **2003**, *15*, 4300–4308.
(15) Talapin, D. V.; Rogach, A. L.; Haase, M.; Weller, H. *J. Phys. Chem. B* **2001**, *105*, 12278–12285.

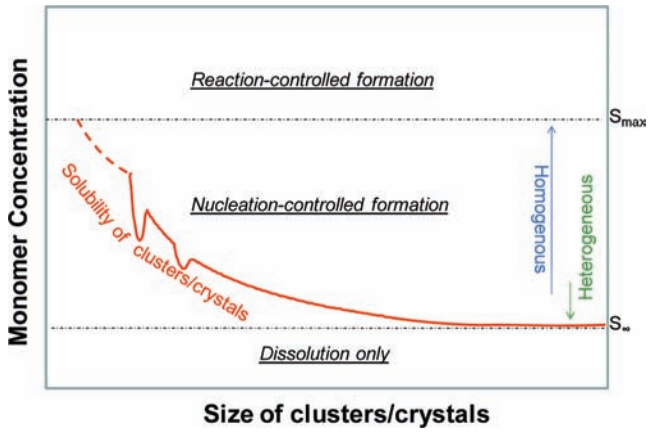

Figure 1. Formation of nanoclusters/nanocrystals. S_{max} and S_∞ at the right side of the plot are the maximum solubility of the clusters/crystals with the smallest possible number of structural units and the bulk crystal, respectively.

only to HSe^- ion, instead of Se^{2-} ions. This shall further reduce the critical sized nuclei calculated using eq 5.

The conclusion drawn in the above paragraph is substantial because it implies that, even from a pure thermodynamic viewpoint, the classic nucleation kinetics might not withstand at all. To better comprehend this conclusion, there are two issues that need to be discussed. It has been well-known that, within 1−2 nm size range, stable nanoclusters are "magic sized clusters", which have a perfect close-shell atomic configuration.[16] Their outstanding stability in comparison to the nanoclusters with similar sizes—either slightly smaller or slightly larger than the given magic size—implies that their solubility should be noticeably smaller than that estimated above (see Figure 1).[12] Furthermore, theoretical and experimental results both revealed that clusters smaller than ∼1 nm are substantially differentiated from the crystal lattice structure. For example, gold clusters up to 18 atoms were found to be flat or hollow cages.[17] This means that the Gibbs−Thompson equation (eq 1) overestimates the equilibrium monomer concentration for very small molecular clusters. In other words, the calculated critical sized nuclei would be further unrealistic in size.

The second issue is regarding experimental observations related to the validity of critical sized nuclei. Molecular dimers and trimers of noble metals, such as Ag_2 and Ag_3, have been observed to form readily in experimental systems by several research groups.[18,19] It is interesting to notice that such molecular clusters could only be isolated under very mild reaction conditions, such as relatively weak visible light and with proper stabilizers in place.[19] Otherwise, formation of large sized crystals would inevitably occur. Furthermore, the results from the Xia group suggested that these tiny molecular clusters determined the final crystal concentration in the solution and could thus be considered as "nuclei" of the system.[18] Such strongly supportive results for stable existence of molecular dimers and trimers have not been observed for the semiconductor nanoclusters/nanocrystal system yet probably because of less interest in this size regime in comparison to the noble metal ones. Fundamentally, noble metal atoms should be extremely insoluble in the reported reaction conditions,[18,19] typically aqueous solutions. Following the same argument offered above, it would be very easy to establish a monomer concentration that is substantially higher than the maximum solubility of such tiny molecular clusters, such as dimers and trimers.

Overall, the above discussions imply that, for very insoluble crystal systems, the monomer concentration in the solution could reach a value higher than the solubility of the smallest possible molecular/cluster species, such as a dimer and trimer. Therefore, in such systems, nucleation kinetics will unlikely play a significant role in the formation of nanoclusters/nanocrystals. Kinetically speaking, this means that the rate-determining step in the formation of such crystals will be chemical reaction(s).

The plot shown in Figure 1 offers a complete picture for the above discussions. In the plot, the red curve is a modified version of the Gibbs−Thompson equation (eq 1). Two possible "magic sized clusters"—presumably between 1−2 nm in size—are represented as two free energy minima in the curve, and the dashed part implies that these molecular clusters (<∼1 nm) have very distinct structures from the bulk crystal and should have substantially smaller solubility than that predicted by the Gibbs−Thompson equation. The maximum solubility (S_{max}) of the system is the solubility of the smallest molecular clusters, possibly a dimer, a trimer, etc., and S_∞ is the solubility of the bulk crystals as defined above. The entire plot area is divided into three regions by S_{max} and S_∞. The bottom region is simply the dissolution of crystals, which does not need to be discussed in this report.

The top region in Figure 1 represents the "reaction-controlled formation" region, in which the monomer concentration in the solution is higher than the maximum solubility of the system. Because of the extremely high supersaturation, formation of clusters/crystals is thermodynamically favorable for all sizes and no thermodynamic barrier exists to define critical sized nuclei. However, because of the existence of the magic sized clusters in the 1−2 nm size range (see the schematic drawing in Figure 1), the initially formed tiny molecular clusters could grow into one of those magic sized clusters and be trapped thermodynamically. This allows us to determine the particle concentration and formation rate of the particles as demonstrated in this work. These nanoclusters could be dissolved *slowly* by the solution additives such as a high concentration of fatty acids, which has been known as "backward tunneling".[12] The condition needed for "backward tunneling" is that the monomer concentration in the solution is below the solubility of the "magic sized cluster", which thermodynamically drives the complete dissolution of the cluster by going through the free energy barrier at the small size side. Alternatively, a high monomer concentration/temperature could help the magic sized clusters to overcome the free energy barrier at their large size side and grow to a large one, which is the "forward tunneling".[12] The combination of "forward tunneling" and "backward tunneling" serve as the basis of "self-focusing" related to nanoclusters.[20]

The middle region in Figure 1 is the "nucleation-controlled formation", which is the main model considered in the classic nucleation literature. In this region, the monomer concentration is lower than the maximum solubility of the smallest molecular clusters in the system but higher than the solubility of the bulk

(16) Herron, N.; Calabrese, J. C.; Farneth, W. E.; Wang, Y. *Science* **1993**, *259*, 1426–1428.
(17) Bulusu, S.; Li, X.; Wang, L. S.; Zeng, X. C. *Proc. Natl. Acad. Sci. U.S.A.* **2006**, *103*, 8326–8330.
(18) Xia, Y.; Xiong, Y. J.; Lim, B.; Skrabalak, S. E. *Angew. Chem., Int. Ed.* **2009**, *48*, 60–103.
(19) Diez, I.; Pusa, M.; Kulmala, S.; Jiang, H.; Walther, A.; Goldmann, A. S.; Muller, A. H. E.; Ikkala, O.; Ras, R. H. A. *Angew. Chem., Int. Ed.* **2009**, *48*, 2122–2125.
(20) Xie, R. G.; Peng, X. G. *Angew. Chem., Int. Ed.* **2008**, *47*, 7677–7680.

crystals. A critical sized nucleus for a given monomer concentration could thus be defined by eq 5 or its variations as discussed above. As a result, formation of a crystal must go through a free energy barrier, which is the homogeneous nucleation accounted by eq 7. As the monomer concentration approaches the solubility of the bulk crystals, homogeneous nucleation needs to overcome a very substantial free energy barrier. Subsequently, heterogeneous nucleation becomes the dominating path, which could be used for growth of hierarchical nanostructures on various substrates.[2]

It should be pointed out that, in this region, initial formation of crystals might still not be nucleation-controlled if there is a very slow chemical process involved (see the first paragraph in this sub-section). In this case, the overall rate of formation would be slower than that predicted by eq 7.

Chemical Kinetics. The chemical kinetics for the "reaction-controlled formation" region in Figure 1 can be empirically presented by eq 12, with k as the reaction kinetics constant and using the InP system studied here as an example.

$$r = \mathrm{d[P]}/\mathrm{d}t = k[\mathrm{In(FA)_3}]^a[\mathrm{P(TMS)_3}]^b[\mathrm{acid}]^c \qquad (12)$$

In Equation 12, a, b, and c are the reaction orders of the corresponding reactants. If some other chemicals are involved in the reaction, more concentration terms should be included. If the reaction obeys Arrhenius kinetics, k can be written as a function of the reaction temperature, activation energy (E_a), and pre-exponential factor (A).

$$k = A\mathrm{e}^{-Ea/RT} \text{ or } \ln(k) = \ln(A) - E_a/RT \qquad (13)$$

The pre-exponential factor in eq 13 is known to be related to activation entropy of a given reaction.[21] Combining eqs 12 and 13, we have the following general equation:

$$\ln(r) = \ln(A) - E_a/RT + a\ln[\mathrm{In(FA)_3}] + b\ln[\mathrm{P(TMS)_3}] + c\ln[\mathrm{acid}] \qquad (14)$$

It should be pointed out that eqs 12, 13, and 14 only account the formation of nanoclusters/nanocrystals. If growth of the crystals is also of consideration, some modifications would be needed. There are some significant distinctions between eqs 7 and 14. For example, the formation rate of nuclei is extremely sensitive to the monomer concentration in eq 7. In the formation of Fe_3O_4 nanocrystals in a similar solvent system used in this work, Kwon et al.[10] estimated that the nucleation rate shall increase 10^{190} by just increasing supersaturation from 2 to 10. This is so because the monomer concentration is in the exponential term in eq 7. Furthermore, eqs 7 and 14 indicates a very different temperature dependence of the formation rate. As described below, these differences are so substantial that it becomes easy to distinguish one type of kinetics from the other.

Experimental Results

Main Reaction System. The main reaction system used in this work was InP nanoclusters/nanocrystal system initiated by injecting tris(trimethylsilyl)phosphine ($P(TMS)_3$) into a hot octadecene (ODE) solution containing indium fatty acid salts and free fatty acid at a given reaction temperature. Fatty acids and the corresponding caroboxylates with different chain length were used widely in this work and also in synthesis of high quality nanocrystals in general. For simplicity, we suggest a unified way to represent them: for a given acid, it would be written as a capitalized "H" combined with the capitalized first letter and the low-case second letter of the common name of the acid. The capitalized "H" will be removed for the corresponding carboxylate. For example, myristic acid and indium myristate should be written as HMy and $In(My)_3$, respectively. This system is consistent with the abbreviation of acetic acid and the corresponding salts. All of the fatty acids used in this work are summarized in the Supporting Information with their abbreviations.

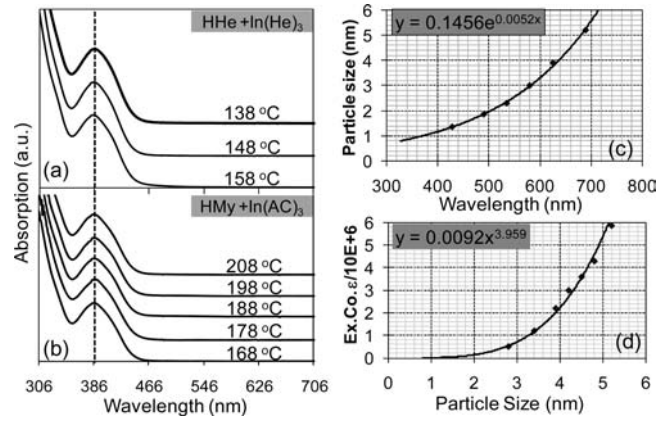

Figure 2. (a) and (b) Absorption spectra of InP nanoclusters formed with different precursors/ligands (HHe = hexanoic acid, HMy = myristic acid) and reaction temperatures. (c) Size dependent absorption peak position of InP nanocrystals adopted from reference with a numerical fitting. (d) Molar particle extinction coefficient of InP nanocrystals vs the size of the nanocrystals adopted from reference.

This choice of the main reaction system was mainly based on the fact that, as shown in Figure 2 (a and b), InP formed small nanoclusters in a quite broad temperature range with different precursors/ligands in this specific reaction system. In addition, unlike typical II−VI semiconductor nanocrystal systems, the involved reaction for the formation of InP in a similar reaction system was identified previously.[22,23] An inorganic salt ($InCl_3$), instead of indium fatty acid salts, was used in the previous reports, and the reaction was proposed as a simple exchange reaction between $P(TMS)_3$ and the indium salt (indium chloride) to yield InP and Cl−TMS. It is reasonable to assume that a similar reaction occurred in the current system.

Because the ligands used were all for cationic surface atoms in the reaction system, all reactions were performed with a large excess of indium precursors unless specified otherwise. Excess indium fatty acid salts helped to maintain colloidal stability of the InP nanoclusters. If a considerable amount of fatty amines were present, however, it was not necessary to maintain an excess amount of indium fatty acid salts.

The size of the nanoclusters shown in Figure 2a and b is slightly larger than 1 nm (Figure 2c) and only has 10−20 structural units (single InP unit) per particle, which should be a "magic sized nanocluster". Their extremely small size makes them be much better qualified as "nuclei" than what have been discussed in the classic theory, greater than tens of nanometers in size.[8] The constant size and size distribution under a broad

(21) Atkins, P. W. *Phys. Chem.*, 6th ed.; 1998.

(22) Micic, O. I.; Sprague, J. R.; Curtis, C. J.; Jones, K. M.; Machol, J. L.; Nozik, A. J.; Giessen, H.; Fluegel, B.; Mohs, G.; Peyghambarian, N. *J. Phys. Chem.* **1995**, *99*, 7754–7759.

(23) Guzelian, A. A.; Katari, J. E. B.; Kadavanich, A. V.; Banin, U.; Hamad, K.; Juban, E.; Alivisatos, A. P.; Wolters, R. H.; Arnold, C. C.; Heath, J. R. *J. Phys. Chem.* **1996**, *100*, 7212–7219.

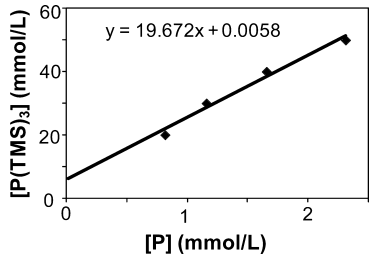

Figure 3. Monomer concentration ([$P(TMS)_3$]) vs InP nanoclusters concentration ([P]). The solid line is a linear fitting of the results with the fitting function in the plot. Reaction conditions: 0.4 mmol $In(He)_3$, 1.2 mmol HHe, 4 mL ODE, $T = 158$ °C.

spectrum of reaction conditions provides two interesting features. First, it largely eliminates experimental errors for determining reaction order and activation energy (see details below). Second, it sets aside the size dependent properties of the nuclei, which could substantially complicate the interpretation of the results because of the drastically different yet unknown relationship between different sized nanolcusters and their supersaturation concentrations. It should be pointed out that formation of such small sized nanoclusters as the initial species is not uncommon. For example, InAs system was actually found to be too difficult to avoid the formation of such nanoclusters in the initial stage.[20]

The extremely small size of the nanoclusters could not be determined directly by transmission electron microscope. Fortunately, both size and molar extinction coefficient (ε) of InP nanocrystals with relatively large sizes were determined by the Weller's group (Figure 2c and d).[24] We carried some additional measurements and found that our results were within the same range. We fitted the data points into numerical functions (Figure 1c and d), which gave us the means to calculate the size and extinction coefficient of the nanoclusters. The size is about 1.1 nm and with about 14 InP units in each nanocluster. From the absorption spectra shown in Figure 2a and b, the InP nanoclusters were unlikely monodispersed. However, the identical peak position and spectral contour indicate that the size and size distribution of the nanoclusters obtained were constant under the reaction conditions specified.

Minimum Concentration of $P(TMS)_3$ for the Formation of InP Nanoclusters. The minimum concentration of $P(TMS)_3$ for the formation of InP nanoclusters was determined under various conditions. Figure 3 illustrates one series of data, which shows that the InP nanoclusters concentration decreased as the initial concentration of $P(TMS)_3$ decreased. The reaction conditions were identical for this set of reactions except the variation of the initial concentration of $P(TMS)_3$. The particle concentration was measured after each reaction proceeded for a sufficient amount of time (~20 s). UV−vis measurements verified that the size and size distribution of the InP nanoclusters in all reactions were almost identical to those shown in Figure 2 (a and b).

The experimental data points in Figure 3 can be well fitted into a linear function (see the fitting function in Figure 3). The fitting line was extrapolated to the particle concentration equals to zero. This gave us the minimum [$P(TMS)_3$] as 5.8 mmol/L, at which no particles could be formed. This value was found to be consistent with the experimental results. Although the particle concentration could not be determined with the same confidence

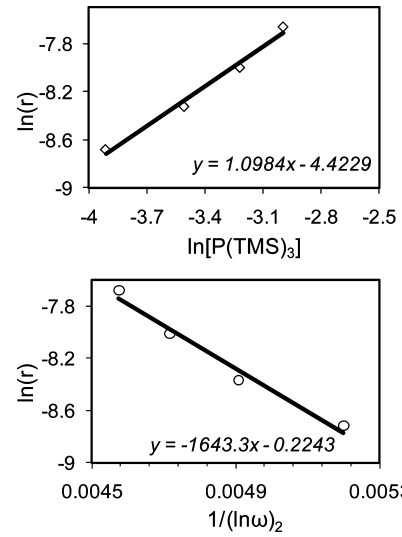

Figure 4. Initial formation rate of nanoclusters vs the concentration of limiting monomer, $P(TMS)_3$. (Top) Plot as chemical kinetics. (Bottom) Plot as classic nucleation kinetics. Reaction conditions: 0.4 mmol $In(He)_3$, 1.2 mmol HHe, 4 mL ODE, $T = 158$ °C.

as the data shown in Figure 3, when [$P(TMS)_3$] was 10 mmol/L, formation of InP nanoclusters was indeed observed. However, when the [$P(TMS)_3$] decreased to 5 mmol/L, InP nanoclusters could not be detected by UV−vis measurements no matter how long time the reaction was maintained.

The existence of a minimum [$P(TMS)_3$] means that, below this concentration, no formation of the nanoclusters occurred in the system under the given reaction conditions. Given the constant size and size distribution of the nanoclusters for all reactions, the minimum [$P(TMS)_3$] could be regarded as the solubility of the given sized nanoclusters. Such an assignment may overestimate the solubility, but it should be at least the upper limit value, which is sufficient for justifying the related analysis later.

With the size and solubility of a given sized nanocluster known, the bulk solubility of InP in the given solution system associated with Figure 3 can be estimated using eq 1 combined with eq 11. Assuming 0.5 J/m^2 as the specific surface free energy[15] and reaction temperature being 451 K, the obtained value for S_∞ is 1.9×10^{-8} mol/L. The solubility values discussed here are all based on the phosphorus monomers. As shown by eq 11, such a relatively high bulk solubility is due to the existence of a decent concentration of free fatty acid, which stabilized the ionization products of InP crystals as H_3P and indium fatty acid salts (eq 9), especially by converting a very unstable P^{3-} to a very stable H_3P.

Reaction Order. The reaction order for the formation of InP nanoclusters was determined for phosphorus precursor, indium precursor, fatty acids, and amines separately. In the reactions without amines added, the $P(TMS)_3$ was the limiting precursor as mentioned above. The top plot in Figure 4 shows that the initial formation rate of the nanoclusters could be well fitted according to eq 14 against the concentration of $P(TMS)_3$. The reaction order can be obtained as the slope of the $\ln(r) - \ln[P(TMS)_3]$ plot, which is practically equal to one. Although the sizes of the CdSe nanocrystals varied from one reaction to another, the previous in situ studies of the formation of CdSe nanocrystals also recorded a first order relationship between the concentration of the nanocrystals and the monomer concentration.[9]

(24) Haubold, S.; Haase, M.; Kornowski, A.; Weller, H. *ChemPhysChem* **2001**, *2*, 331.

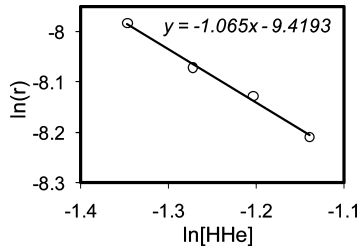

Figure 5. Initial formation rates of the InP nanoclusters vs the acid concentration (HHe). Reaction conditions: 0.4 mmol $In(He)_3$, 0.2 mmol $P(TMS)_3$, 4 mL ODE, $T = 158$ °C.

The discussion in the above paragraphs also reveals that the increase of the formation rate of nanoclusters as the increase of the monomer concentration would be too slow to be explained using the classic nucleation theory. To further illustrate this point, the experimental results were replotted (Figure 4 bottom) using the nucleation kinetics equation (eq 7a). The supersaturation (ω) for a given reaction was calculated by using the bulk solubility measured against [$P(TMS)_3$] (see Figure 2 and the related text). The fitting was slightly worse than that using eq 14. The pre-exponential factor (A) for the nucleation kinetics was calculated as 1.24 using the intercept in the plot (see eq 7a), which is unreasonably small for a solution reaction. The most striking discrepancy was found for the slope of the fitting. From the slope of the plot (Figure 4, bottom), the specific surface free energy was calculated to be 25 000 000 (J/m^2), which is about 7 magnitudes larger than what could be expected.[15] The bulk solubility estimated above (see Figure 2 and the related text) was an upper limit value. By referring to eq 7, one would expect an even larger discrepancy using a lower bulk solubility in calculating supersaturation. In any case, such a large discrepancy was often noticed in literature,[6] which implies that the nucleation kinetics equation does not work for the current system.

The concentration effect of indium precursors was found to be small in the reactions without the addition of amines because such reactions needed to be run under excess indium precursor conditions. With a large excess of amine in place, the formation rate of InP nanoclusters was determined to be the third order against the concentration of indium precursors (Figure S1, Supporting Information). The existence of amines also affected the reaction order of $P(TMS)_3$, from the first order without amine (Figure 4, top) to the second order with amine (Figure S2, Supporting Information). As discussed below, the sizes of the InP nanoclusters were found to be less constant and slightly larger than the ones shown in Figure 2 (see detail below). However, although the reaction orders were different for the reactions with and without amines, the general conclusion was the same, that the formation kinetics could be well fit with the regular chemical kinetics (eq 14), instead of nucleation kinetics (eq 7).

The reaction order of additives for the formation of nanoclusters was also studied. Fatty acids have been widely used as an additive in synthesis of high quality colloidal nanocrystals in organic solvents after the introduction of the "greener approaches".[4] It was found that, for the case of CdS nanocrystals,[13] fatty acids reduced the consumption rate of precursors in the nucleation stage but not the growth stage. Consistent with this, the results in Figure 5 reveal that, for InP q-dot system, the formation rate of the given sized nanoclusters was found to be inversely proportional to the acid concentration, negative one as the reaction order. It should also be pointed out that, if no amines were added in the reaction solution, changing the concentration of fatty acids did not change the size and size distribution of the InP nanoclusters. Because the reaction order was negative one, fatty acids should promote the dissolution of the InP nanoclusters, or the "backward tunneling" of the nanoclusters discussed above.[12] Consistent with this, this dissolution process seemed to be quite slow. For the reaction with the highest acid concentration in Figure 5, if the reaction was allowed to proceed for about 20 min or longer, the nanoclusters would gradually disappear. Furthermore, in all reactions, if a significant amount of fatty acid was added after the formation of the InP nanoclusters, the nanoclusters could be completely dissolved slowly.

The amine-added reactions yielded large InP nanoclusters with some variation in their size and size distribution (see details below). The reaction rate for the formation of the InP nanoclusters did not show a monotonic trend against the amine concentration (Figure S3, Supporting Information). This was not considered to be completely surprising. In literature, the roles of fatty amines were found to be complex, including formation of a complex with indium ions to slow down the reaction rate, activation of metal fatty acid salts through the formation of amides, coordination to the surface of the nanoclusters/nanocrystals, formation of salts with fatty acids to indirectly activate the reaction, etc. Presumably, by changing their concentration, each of these roles of amines may have a different weight in the whole reaction scheme, which ended up a nonmonotonic relationship between the formation rate of the nanoclusters and the concentration of the amines. In addition, these complex roles could also complicate the reaction paths and might cause the dramatic change of the reaction orders against the precursors discussed above.

Temperature Dependence of the Formation Rate of the InP Nanoclusters. The temperature dependence of the formation rate of the InP nanoclusters was determined under a variety of conditions. Figure 6 illustrates the results for the reactions without the addition of amines by varying the chain length and concentration of the fatty acids. The experimental results could be well fitted with the chemical kinetics equation (eq 14). In such a $\ln(r) - 1/(RT)$ plot, the activation energy can be obtained as the slope of the linear fitting as shown by eq 14. To maintain the same nanocluster size and size distribution, the reaction temperature ranges may differ from one series to another. According to eq 14, however, this should not affect the determination of the activation energy (E_a).

The activation energy was found to be the same in the reaction series for the same type of fatty acid with different acid concentrations, namely, 6.3 ± 0.3 (KJ/mol) for butaoic acid, 9.1 ± 0.3 (KJ/mol) for hexanoic acid, and 10.7 ± 0.3 (KJ/mol) for octanoic acid. This means that the activation energy increased as the increase of the chain length of the acids (Figure 6, right).

Although the activation energy was the same for the same type of acid by varying the acid concentration (see Figure 6 left and middle plots as examples), the intercept decreased systematically as the acid concentration increased. This matched the reaction order well for fatty acid determined above (Figure 5). According to eq 14, for a given type of acid, the difference between two different acid concentrations in Figure 6 should only be the acid concentration term, $-\ln[\text{acid}]$. Because the reaction was found to be negative first-order against fatty acid concentration (Figure 5), the difference of the y-axis intercepts between two lines in Figure 6 (either left or middle plot) could

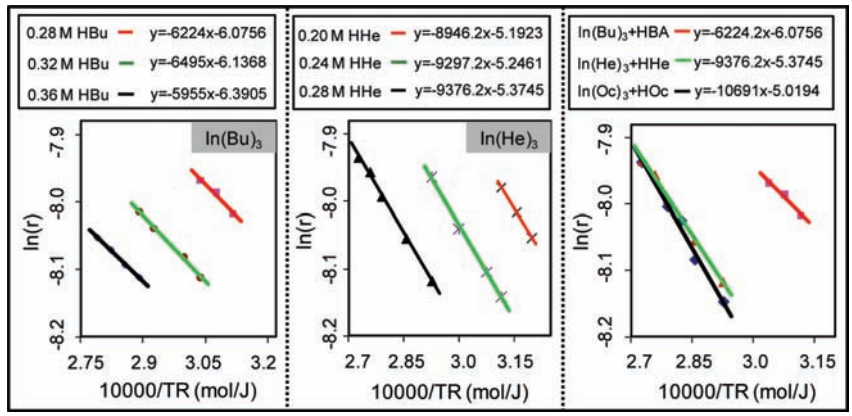

Figure 6. Irving plots of the initial formation rate of the InP nanoclusters without amine in place. (Left) Reactions with indium butanate ($In(BA)_3$) as the precursor and different buranoic acid concentrations. (Middle) Reactions with indium haxanate ($In(HA)_3$) as the precursor and different hexanoic acid concentrations. (Right) Reactions with the acids of different chain-length but the same acid concentration. In all experiments, $[In(FA)_3] = 0.08$ mol/L, $[P(TMS)_3] = 0.04$ mol/L.

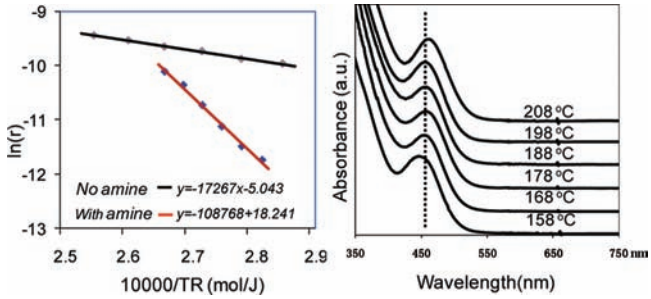

Figure 7. (Left) Irving plot of the reactions with and without fatty amines added. (Right) Absorption spectra of the InP nanoclusters formed at different reaction temperatures with amine added. Reaction conditions: 0.4 mmol $In(Ac)_3$, 0.2 mmol $P(TMS)_3$, 1.5 mmol HMy, 4 mL ODE.

be readily calculated. The calculated values matched quite well with the fitting results.

If the formation of the InP nanoclusters followed the classic nucleation kinetics (eq 7), one should not expect the results shown in Figure 6. The increase of acid concentration shall substantially increase the bulk solubility (eq 11), which means that the supersaturation should decrease as the concentration of acid increased. For example, when hexanoic acid concentration increased from 0.20 to 0.28 mol/L without changing the other reaction conditions (Figure 6, middle), one can calculate that the supersaturation decreased by 2.7 times, estimated using eq 11. This should be reflected as a significant change of the slope in the plot, instead of being constant (Figure 6 left and middle). Furthermore, according to eq 7a, the intercept should not change upon changing the acid concentration for nucleation-controlled formation. These facts imply that, similar to the results on the reaction orders discussed above, the temperature dependence of the formation rate of the InP nanoclusters supported the reaction-controlled mechanism, instead of classic nucleation-controlled mechanism.

The temperature dependence of the reactions using indium acetate ($In(Ac)_3$) as the indium precursor was also studied by varying the ligand (myristic acid) concentration (Figure S4). $In(Ac)_3$ and other types of metal acetates are the commonly available metal-organic compounds and have been widely used directly as the metal precursors for synthesis of high quality nanocrystals. Because of the very short hydrocarbon chain, long-chain fatty acids with different concentrations are often added as the ligands of the resulting nanocrystals. The exact composition of the metal fatty acid salts, however, was found to vary substantially.[25] As a result, the activation energy and pre-exponential factors also changed significantly (Figure S4, Supporting Information), reflecting a different reaction path. This means that, if mixed ligands are used in a synthesis, the exact precursor structure shall affect the formation kinetics substantially.

Temperature Dependence of the Reactions with Fatty Amines Added As Additives. The temperature dependence of the reactions with fatty amines added as additives was also studied. The size of the nanoclusters formed with amine added (Figure 7 right) was found to be larger and less constant under different reaction temperatures than those generated in the reactions without amines (Figure 2).

The results in Figure 7 (left) indicate that the addition of amines in this temperature range increased the activation energy substantially, which experimentally resulted in a significant increase of the temperature dependence of the formation rate of the InP nanoclusters. The pre-exponential factor also increased upon the addition of the amines. These results could be tentatively explained by the fact that fatty amines were found to stabilize indium ions in nonpolar solvents under the reaction conditions.[26] A stable complex should increase activation energy by decreasing the potential energy of the reactants. Because amines are neutral ligands, the charges of the indium ions must be balanced by the carboxylates. As a result, the indium precursor becomes very complex in comparison to the original indium fatty acid salts. When the transition state was formed by the reaction of this complex indium precursor with the phosphorus precursor, the activation entropy would be quite large by releasing more molecules into the reaction solution. Therefore, by adding fatty amines into the reaction system, an increase of the activation entropy should be expected, which in turn increased the pre-exponential factor according to the Eyring's equation.[21]

The above interpretation implies that fatty amines "activate" metal fatty acid salts by increasing the activation entropy, instead of decreasing the activation energy. Consistent with this, although InP nanoclusters could be formed at a temperature below 100 °C without the presence of amine, the reactions with amines did not show appreciable formation of InP particles at

(25) Narayanaswamy, A.; Xu, H.; Pradhan, N.; Kim, M.; Peng, X. *J. Am. Chem. Soc.* **2006**, *128*, 10310–10319.
(26) Koo, B.; Patel, R. N.; Korgel, B. A. *J. Am. Chem. Soc.* **2009**, *131*, 3134–3135.

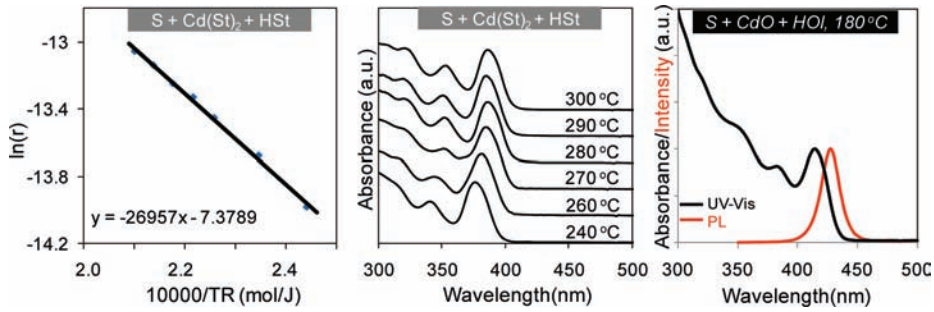

Figure 8. Arrhenius plot of the formation of CdS nanocrystals (left) and the corresponding absorption spectra (middle). UV−vis and photoluminescence (PL) spectra of as-synthesized CdS nanocrystal sample grown at 180 °C (right) using oleic acid (HOl) as the ligands and CdO as the Cd precursor.

such relatively low temperatures. At a high reaction temperature, however, the reaction rate for the amine-based reactions enhanced substantially, which promoted a rapid growth of the relatively large InP nanocrystals in amine-based reaction systems.[27]

CdS Nanocrystals System. The CdS nanocrystals system was studied to examine the possibilities to extend the above experimental strategies to other crystallization systems. Similar to the InP system without amines added, CdS nanocrystals could be formed with cadmium fatty acid salts (such as cadmium stearate, $Cd(St)_2$) and elemental S in ODE with fatty acid added as the only additive.[13] For this well developed system, it was possible to form nearly monodisperse CdS nanocrystals with a relatively large size (~2.8 nm) in a quite broad temperature range (Figure 8, middle).

The reaction order for the formation of the CdS nanocrystals against the rate limiting precursor, S, was found to be 2 (Figure S5, Supporting Information). The results in Figure 8 (left) show that the activation energy for the formation of CdS nanocrystals under the specified reaction conditions was about 27 kJ/mol. All of these results indicate that this system can also be well described using the reaction-controlled formation. Furthermore, the relatively low activation energy implies that CdS nanocrystals could be synthesized at a temperature much below the typical temperature used for this established reaction system, between 250 and 300 °C.[13] Preliminary results indeed confirmed that high quality CdS nanocrystals could be synthesized at 180 °C (Figure 8, right).

Discussion

Accuracy. The accuracy on determining the size, shape, size/shape distribution, and concentration of the initial solid seeds (nuclei) has been the main obstacle for studying nucleation process. The results reported here indicate that, under carefully chosen reaction conditions, it would be possible to solve this problem by taking advantage of the size-dependent optical properties of semiconductor nanocrystals/nanoclusters. However, although it has been possible to generate nanocrystals with a good control over the size and size distribution, some uncertainty on these structural parameters shall still exist.

The experimental method demonstrated a possibility to study formation of nanoclusters/nanocrystals with a fixed size and size distribution. In this method, any inaccuracy on determining the size, size distribution, and extinction coefficient would be eliminated for determining the reaction order and activation energy. This is so because any inaccuracy on these parameters will end up as a systematic error for the intercept of an Arrhenius plot and not affect the slope of the linear plot. Equation 14 indicates that activation energy and reaction orders are solely determined by the slope of the plots under different reaction conditions. For the intercept, its absolute value may not be accurate but the difference between the intercepts of two linear fitting functions (see Figures 6 and S4, Supporting Information) should still be reliable because systematic errors would be canceled in calculations of difference.

The reaction rates presented here were all initial reaction rates, which were calculated by measuring the samples taken at 5 s after the initial injection of the phosphors (or sulfur) precursor solution into the reaction solution. The injection/mixing process took approximately 1 s, and the fastest sampling was about 5 s manually. The samples were taken with a time inaccuracy of about 1 s. Evidently, the improvement of accuracy of this method, that is, determination of formation rates with fixed size and size distribution, should come from the measurement of the reaction time, such as an in situ scheme for recording the absorption spectra. In fact, previous in situ studies[9] indicate that formation of CdSe nanocrystals in a similar reaction system could last for a few seconds, which means that the current time accuracy might not be too bad.

Reaction-Controlled Kinetics, Instead of Nucleation-Controlled Kinetics. The reaction-controlled kinetics, instead of nucleation-controlled kinetics seemed to be consistent with the experimental data. As mentioned above, this implies that chemical reactions should be the rate-determining step in the systems studied here. According to Figure 1 and the related discussions, "reaction-controlled formation" might generally be the dominating path for the synthesis of high quality colloidal nanocrystals. This is so for two reasons. First, nearly all of the targeted nanocrystal systems today are extremely insoluble ones in solvents. Second, when a synthetic scheme was developed, the precursor concentrations have always been pushed to a high limit to achieve a high yield in synthesis. These two factors could allow a system to readily reach an extremely high supersaturation to justify the "reaction-controlled formation", instead of the "nucleation-controlled formation" (Figure 1).

The question is why nucleation—corresponding to "nucleation-controlled formation" in Figure 1—has historically been well accepted as the central concept for the formation of crystals although this region seems to be just one part of the picture. For crystals with a reasonably high solubility, such as NaCl or other highly soluble salts in water, the S_{max} corresponding to those molecular clusters could be too high to reach for a practical solution. As a result, "reaction-controlled formation" would become forbidden. Furthermore, if the solubility is too high, homogeneous nucleation might also become very difficult to

(27) Xie, R.; Battaglia, D.; Peng, X. *J. Am. Chem. Soc.* **2007**, *129*, 15432–15433.

observe and heterogeneous nucleation (see Figure 1) shall dominate the system as noticed by Mullen in his famous book.[5]

There is a reason that causes people to believe nucleation is a universal picture, even for very insoluble crystals. As discovered recently, when the concentration of nanocrystals/nanoclusters reached a certain value, "self-focusing"[20,28,29] (see Theoretical section) might start to occur if the nanoparticles are somewhat soluble in the solution with the existence of relatively strong ligands. This process shall stop the further formation of crystals, which could be mis-interpreted as the completion of nucleation. On the other hand, if the crystals were nearly completely insoluble, initial formation of crystals would be very fast and stop sharply because of the depletion of monomers. This may be mis-regarded as the completion of nucleation as well.

It should be pointed out that "magic sized clusters" have often been mistaken as the critical sized nuclei, at least in synthesis of semiconductor nanocrystals.[12] However, the model in Figure 1 tells us that these local thermodynamic minima could just be shallow traps in a crystallization system. Inconsistent with the expectation of critical sized nuclei, further growth of "magic sized clusters" requires the clusters to overcome a thermodynamic barrier, namely the barrier on the right side in each potential trap associated with "magic sized clusters" in Figure 1. Thus, addition of a few structural units to the clusters is thermodynamically unfavorable, which is why the growth of a "magic sized cluster" has always been observed to end up a much larger nanocrystal—"forward-tunneling". Consequently, the growth of "magic sized clusters" has been observed to be slow.[12,20] However, if these nanoclusters are qualified as critical sized nuclei, the classic nucleation theory[12] would require the formation of the "magic sized clusters" to be slow and the following growth to be much faster, which is opposite to the experimental results.

Growth of Nanoclusters/Nanocrystals. The growth of nanoclusters/nanocrystals after their formation is likely size dependent. For example, as mentioned in the above paragraph, the growth of "magic sized clusters" was found to be particularly slow. In addition, several known phenomena observed in the growth stage, such as Ostwald ripening, intraparticle ripening, and "self-focusing", are all direct results of the size dependent chemical stability (reactivity) of the nanoclusters/nanocrystals. This implies that theoretical treatment of the growth of nanoclusters/nanocrystals probably should not ignore the size dependent chemical properties of the particles although the formation process—nucleation in traditional meaning—could concentrate on the initial chemical reaction(s).

Experiment Section

Materials. Technical grade (90%) Octadecene (ODE), Indium acetate (In(Ac)3, 99.99%), Stearic acid (98%), Myristic acid (99%)Butyric acid (99%), Hexanoic acid (98%), Octanoic acid (90%), Tris-trimethylsily phosphine ($P(TMS)_3$, 95%), 1-octylamine (99%) were purchased from Alfa. All indium fatty acid salts were prepared in our lab by using the same method reported in literature.[28] All the chemicals were used without further purification.

Synthesis of InP Nanocrystals/Nanoclusters without Amine. The injection solution of P precursor was prepared by mixing tris-trimethylsilyl phosphine and ODE (1.0 mL in total) in a glovebox. For a typical synthesis, $In(He)_3$ (0.4 mmol), hexanoic acid (1.4 mmol), and 4 g of 1-octadecene (ODE) were loaded into a three-neck flask. The mixture was heated to 18 °C under argon flow, and then, the P precursor solution made in glovebox was injected into the hot reaction mixture. For determining the initial reaction rate, an aliquots was taken immediately (5 s) after the injection. The concentration of InP nanocrystals in reaction was calculated using the Beer's law by measuring the diluted solution of the aliquots. To determine the concentration reproducibly, the amount of reaction mixture was measured using an analytical balance by mass, while the direct record of volume of the aliquots was found to be inaccurate.

Synthesis of InP Nanocrystals/Nanoclusters in Presence of Amines. The injection solution of the P precursor was prepared by mixing tris-trimethylsilyl phosphine and 2.4 mmol octylamine in ODE (1.0 mL in total) in a glovebox. For a typical synthesis, indium acetate (0.4 mmol), myristic acid (1.4 mmol), and 4 g of 1-octadecene (ODE) were loaded into a three-neck flask. The mixture was heated to 178 °C under argon flow, and then, the P precursor solution made in glovebox was injected into the hot reaction mixture. The rest of the procedures were the same as those described above.

Composition of the Indium Fatty Acid Salts. The composition of the indium fatty acid salts in the reactions using indium acetate plus a long chain fatty acid was determined using FTIR method. In a typical reaction, 0.4 mmol indium acetate, 1.25 mmol myristic acid and 4 mL ODE were loaded into flask. The mixture was heated to 188 °C under argon. The sample of the mixture was taken for FTIR measurement after 5 min. The amount of acid in a given mixture was determined using a standard myristic acid solution with known molar concentration in ODE.

Synthesis of CdS Nanocrystals. The synthesis of CdS nanocrystals followed a similar method reported in literature.[13] For determining the activation energy, ODE (4 mL), 0.4 mmol $Cd(St)_2$ and 0.2 mmol SA were loaded into three-neck flask. The mixture was heated to a given temperature in the range between 240 and 300 °C under argon, then 0.2 mmol S in ODE was injected quickly into the reaction mixture. An aliquots was taken immediately taken (about 5 s after the injection) for the measurements of UV−vis spectrum. The particle concentration was determined using the same method for the InP nanoclusters/nanocrystals system discussed above with the extinction coefficients in literature.[30]

Acknowledgment. This work was partially supported by the NSF and NIH.

Supporting Information Available: Table of fatty acids, reaction orders of indium precursor, amines, and sulfur (for CdS system), as well as the temperature dependence of the formation rate of InP using $In(Ac)_3$ as the precursor. This material is available free of charge via the Internet at http://pubs.acs.org.

JA9063102

(28) Chen, Y.; Johnson, E.; Peng, X. *J. Am. Chem. Soc.* **2007**, *129*, 10937–10947.
(29) Thessing, J.; Qian, J.; Chen, H.; Pradhan, N.; Peng, X. *J. Am. Chem. Soc.* **2007**, *129*, 2736–2737.
(30) Yu, W. W.; Qu, L.; Guo, W.; Peng, X. *Chem. Mater.* **2003**, *15* (14), 2854–2860.